

## Optimized Convolutional Neural Networks and Binary Chimp Feature Selection for Robust Medicinal Plant Image Classification

Chen Yu<sup>1</sup>, Li Qiang<sup>1</sup>, Zhang Wei<sup>1</sup>, Sun Hao<sup>1\*</sup>

<sup>1</sup>Department of Digital Health, School of Medicine, Tsinghua University, Beijing, China.

\*E-mail ✉ [sunhao@tsinghua.edu.cn](mailto:sunhao@tsinghua.edu.cn)

Received: 10 March 2022; Revised: 29 May 2022; Accepted: 02 June 2022

### ABSTRACT

This study emphasizes the importance of medicinal plants as a key component of global biodiversity conservation and human health. It specifically stresses the necessity for precise identification of medicinal plant species to ensure their sustainable protection and proper application. Traditional classification techniques face difficulties due to the intricate nature of plant characteristics and the scarcity of annotated datasets. To overcome these limitations, this work introduces a deep learning–driven model for recognizing medicinal plant images using Convolutional Neural Networks (CNNs). The framework utilizes a CNN design integrating both residual and inverted residual blocks, supported by extensive data augmentation to strengthen the dataset. For feature selection, the system employs Binary Chimp Optimization in combination with serial feature fusion to enhance both accuracy and computational speed. Experimental findings indicate that the proposed method markedly surpasses conventional classification techniques in identifying medicinal flora, and it provides a strong foundation for future extensions to other plant groups. Overall, the results demonstrate how deep learning architectures can significantly advance automated plant identification when paired with botanical research.

**Keywords:** Medicinal plant, Classification, CNN, Chimp optimization, Feature fusion

**How to Cite This Article:** Yu C, Qiang L, Wei Z, Hao S. Optimized Convolutional Neural Networks and Binary Chimp Feature Selection for Robust Medicinal Plant Image Classification. *Interdiscip Res Med Sci Spec.* 2022;2(1):140-51. <https://doi.org/10.51847/RuKuk19qZi>

### Introduction

Medicinal plants represent an essential resource for global healthcare, contributing significantly to both traditional therapies and modern pharmaceutical development. Reports from the WHO estimate that 35,000–70,000 plant species are used medicinally, accounting for roughly 14–28% of the 250,000 plant species known worldwide and 35–70% of plant usage overall [1, 2]. Approximately 70% of the world’s population relies primarily on plant-based remedies for healthcare needs [3]. Their importance stems from diverse bioactive compounds capable of producing therapeutic effects in humans [4, 5]. Many culturally important medicinal plants are integrated into daily diets and traditional healing practices, contributing to local economies and livelihoods [6]. In response to their ecological and social value, several global guidelines have been established for the protection of medicinal plant biodiversity [7].

Given their significance, accurate species identification is vital both for conservation initiatives and for preserving traditional knowledge systems. Yet manual identification methods are often unreliable, as many species closely resemble one another. Advances in computer vision and machine learning have enabled automated plant recognition tools. Widely known apps such as LeafSnap and Pl@ntNet illustrate the potential of these technologies, though they still struggle with variations in plant morphology, including differences in leaf form, color, and texture. Consequently, deep learning–based techniques have been developed to enhance classification accuracy [8–10].

Deep learning, especially CNN-based models, has become the dominant approach for image recognition tasks, outperforming earlier machine learning systems that depend on handcrafted features. CNNs automatically learn

hierarchical feature representations, which improves their effectiveness in complex classification tasks such as plant species identification [11, 12].

Recent developments have shifted attention toward hybrid systems that integrate multiple deep learning architectures. Hybrid transfer learning approaches have shown strong performance, particularly in medicinal plant classification. For instance, Ghosh *et al.* [13] demonstrated that combining PCA with CNNs produced 95.25% test accuracy—higher than many prior models. Such hybrid approaches address problems like high feature dimensionality and extensive training requirements, making them feasible for practical scenarios. Despite notable progress, research gaps remain, especially regarding systems that integrate multiple architectural components such as residual blocks, inverted residual blocks, and feature fusion. Existing models often assume large labeled datasets and high computational resources, which are not always accessible. Furthermore, limited work has been directed toward real-world applications that benefit local communities and practitioners.

To address these challenges, our work introduces a hybrid deep learning framework for medicinal plant recognition. The model utilizes both residual and inverted residual block architectures to extract rich visual features. These features are optimized using the Binary Chimp Optimization (BCO) algorithm for dimension reduction and selection of the most informative attributes. Additionally, a feature fusion strategy merges the strongest features from both architectures to enhance classification performance.

Model interpretability is further improved by applying Grad-CAM (Gradient-weighted Class Activation Mapping), which highlights image regions that influence classification decisions. The main contributions of this study include:

- Applying extensive data augmentation to improve the diversity and generalization of the training set.
- Designing a hybrid CNN architecture combining residual and inverted residual blocks for comprehensive feature extraction.
- Implementing a feature fusion mechanism that integrates context-rich features from both architectural streams.
- Utilizing BCO for selecting the most discriminative features, thereby increasing accuracy and reducing computation time.
- Deploying machine learning classifiers on the optimized feature set to achieve highly accurate medicinal plant classification.
- Using Grad-CAM visualizations to identify critical regions in plant images and enhance the interpretability of the model's predictions.

The structure of the paper is as follows: Section 2 reviews related research on medicinal plant classification and hybrid deep learning methods. Section 3 details the system architecture, including preprocessing, feature extraction, and classification techniques. Section 4 presents experimental results, evaluation metrics, and comparisons with existing models. Finally, Section 5 summarizes the findings and outlines future research prospects.

### *Related works*

Over recent years, progress in plant leaf recognition and disease diagnosis has accelerated due to advances in computer vision and machine learning. Current studies span classical image-processing pipelines to modern deep learning architectures, each contributing to improvements in precision and stability for species classification and disease detection. The works summarized below outline developments in feature extraction, classification strategies, and preprocessing methods tailored to leaf-based analysis, illustrating the wide range and versatility of present methodologies used in plant identification.

### *Traditional plant leaf classification methods*

Classical computer-vision techniques have long been applied to distinguish plant species and detect leaf disorders, with hand-crafted features serving as the basis for categorization. Wu *et al.* [14] extracted twelve shape-related descriptors derived from five geometric properties and used PCA to compress dimensionality before sending the reduced vectors to a probabilistic neural network. Using their own Flavia dataset, they reported an overall accuracy of 90.3%. Herdiyeni and Wahyuni [15] achieved 74.5% accuracy by merging fuzzy local binary patterns, fuzzy color histograms, and a PNN classifier on a set of 2448 leaf samples (resolution  $270 \times 240$  pixels) collected from Indonesian medicinal flora. Ma *et al.* [16] combined Pyramid Histograms of Oriented Gradients (PHOG), Haar wavelet features, and a Top-hat transform, achieving 90% performance on ImageCLEF 2012 leaf images.

### *Deep learning models for plant leaf classification*

As deep learning became prominent, manual feature design was gradually replaced by models capable of learning representations automatically. Grinblat *et al.* [17] attained 92% accuracy when classifying leaves from three species using a CNN with three convolutional layers focused on venation structures. Paulson and Ravishankar [18] categorized 64 medicinal plant species using three CNN setups—VGG16, VGG19, and a custom architecture—achieving 95.7%, 97.8%, and 97.6% accuracy, respectively. Nasiri *et al.* [19] showed that CNN models applied to visible-light data (400–700 nm) could distinguish grape leaf cultivars with 99% accuracy across six varieties. Hu *et al.* [20] developed a Multi-Scale Function (MSF) CNN that integrates multiscale learning branches for leaf identification. Experiments on the MalayaKew (MK) and LeafSnap datasets demonstrated that their MSF-CNN achieved top-tier performance relative to comparable systems.

### *Hybrid models and optimization techniques*

Recent investigations highlight hybrid strategies in which CNNs are coupled with optimization heuristics to enhance performance. Ghosh *et al.* [13] presented a Parallel Big Bang–Big Crunch (PB3C)-based CNN framework, using PB3C to tune CNN architecture parameters for improved accuracy and efficiency. They further introduced the HPB3C-3PGA algorithm, integrating PB3C with the 3-Parent Genetic Algorithm (3PGA) to accelerate the search for optimal CNN structures. This hybrid system provides broad exploration capabilities while retaining global convergence properties, ultimately producing higher accuracy with lower computational cost. These efforts reflect growing interest in merging CNNs with metaheuristic optimizers for large-scale classification scenarios.

### *Challenges and opportunities*

Although performance has advanced considerably, several issues remain. Significant intra-class variability—stemming from lighting differences, occlusion, and natural morphological changes—continues to impair model reliability when dealing with medicinal plants. To counter this, data augmentation (e.g., rotations, flips, noise injection) is commonly used to make models more resilient. Hybrid optimization schemes like HPB3C-3PGA show promise in addressing architecture-selection challenges by combining multiple search strategies to avoid local optima and accelerate convergence. Building on this direction, our study incorporates Binary Chimp Optimization (BCO) alongside CNN models to further boost classification accuracy.

### *Summary of key contributions*

This research extends contemporary classification frameworks by employing a hybrid strategy tailored for medicinal plant recognition. The major contributions include:

- Integration of Inverted Residual and Residual Blocks: This design enhances the feature-extraction stage, improving both model stability and accuracy.
- Use of Binary Chimp Optimization (BCO): BCO identifies the most informative feature-map components so that only essential descriptors are passed to the classifier.
- Serial-Level Feature Fusion: Features from all network modules are aggregated sequentially, yielding richer representations and markedly improved performance.

Incorporating these elements aligns our method with recent advancements, such as those by Ghosh *et al.* [13], while addressing gaps by offering a complete, end-to-end medicinal plant classification pipeline combining state-of-the-art CNN structures with an efficient optimization strategy.

### *Proposed methodology*

**Figure 1** illustrates sample medicinal plant images used in this study. The workflow begins with data augmentation performed on the selected dataset (**Figure 2**). After augmentation, the expanded dataset is processed through two custom model streams built using inverted residual designs and a self-attention framework (**Figure 3**). Feature sets from the self-attention pathway and the inverted-residual-based model are extracted and then merged using a sequential fusion technique (**Figure 4**). The fused features are subsequently refined by the Binary Chimp Optimization method to select the most discriminative attributes. Finally, Grad-CAM visual explanations are applied to highlight diseased or healthy regions on the leaf samples. The following section describes each stage in detail.

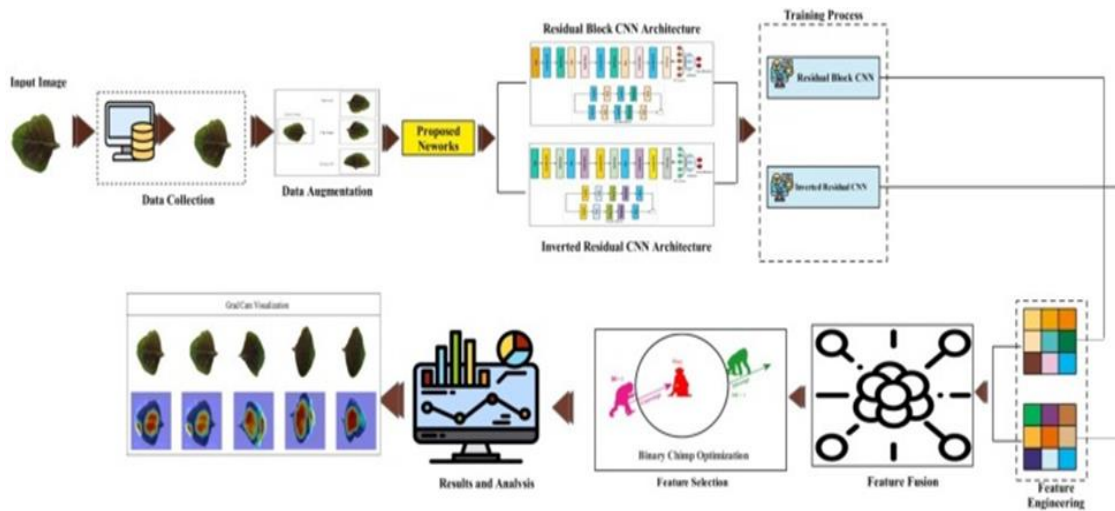


Figure 1. Proposed architecture for medicinal plant classification.

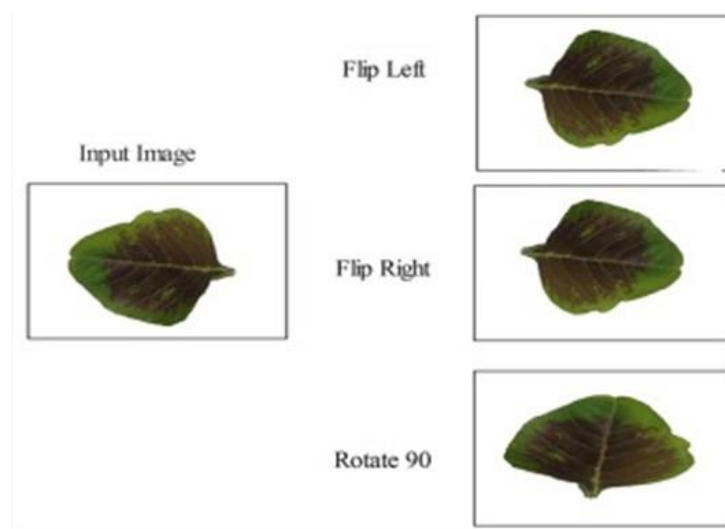


Figure 2. Data augmentation steps.

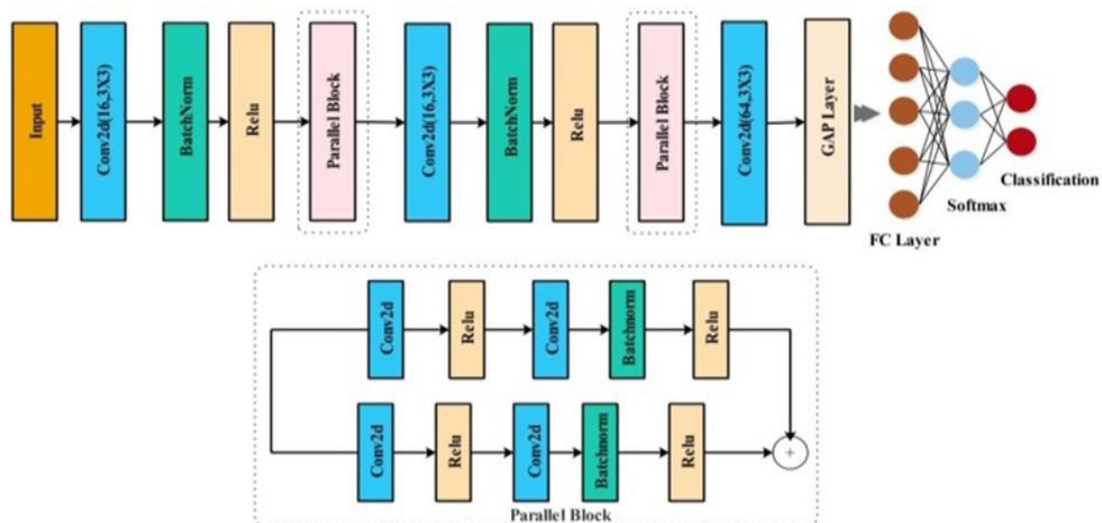
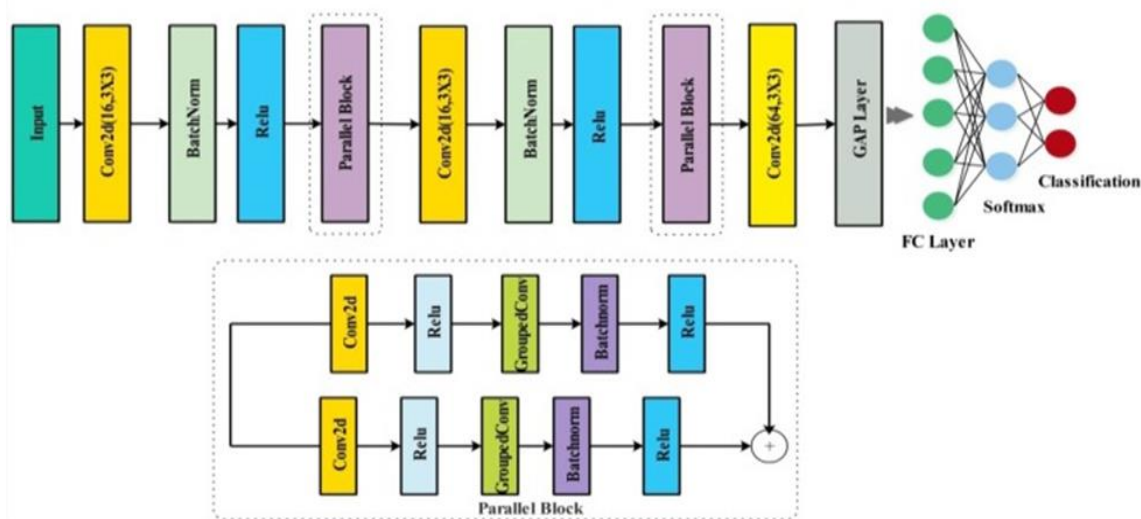


Figure 3. Design of the proposed residual block.



**Figure 4.** Design of the proposed inverted residual block.

#### *Dataset collection and augmentation*

This study employs a publicly accessible medicinal plant image dataset from Kaggle (<https://www.kaggle.com/datasets/sharvan123/medicinal-plant>), which contains 30 classes. Since the dataset is inherently imbalanced, augmentation is necessary to improve training quality. The dataset used for validation consists of 1000 images, each with an approximate resolution of  $500 \times 500$  pixels. The collection is divided evenly into training and testing subsets.

Due to the limited number of samples, the raw dataset alone is insufficient for training deep networks. As illustrated in **Figure 2**, augmentation techniques—Left Flip, Right Flip, and  $90^\circ$  Rotation—are applied repeatedly across all classes until an adequate number of examples is obtained for model training.

#### *Proposed residual block architecture*

The Residual Block is a crucial component of MobileNetV2, a lightweight CNN widely used in mobile and embedded vision tasks due to its reduced computational load and strong performance. This work utilizes a dual-parallel residual block design (**Figure 1**). The CNN structure adopts an inverted residual block format and receives input images sized  $224 \times 224 \times 3$ .

Following the input, the model applies a convolution layer with  $3 \times 3$  kernels, a depth of 16, a  $2 \times 2$  stride, and batch normalization. The first parallel branch contains two convolution layers with batch normalization and ReLU, using  $3 \times 3$  kernels, depth 16, and a  $1 \times 1$  stride. The second inverted residual branch contains two convolution layers and batch normalization with a depth of 32, also using a  $3 \times 3$  kernel and  $1 \times 1$  stride, together with ReLU activation.

Additional skip connections link the grouped convolution to the fully connected layer, softmax, global average pooling, and final classifier. The entire model includes approximately 258k parameters, with 22 out of 45 layers being convolutional ones. The deep features following global average pooling are removed, and the model is trained on both datasets. The resulting feature dimension is  $N \times 1024$ . The full architecture of the residual-based CNN is shown in **Figure 3**.

#### *Proposed inverted residual block architecture*

The alternative design in this framework uses a CNN architecture built from three parallel blocks based on an inverted residual structure. As in the previous model, the input size is  $224 \times 224 \times 3$ . After receiving the input, the network applies batch normalization and a convolution layer with a  $3 \times 3$  kernel, 16 filters, and a  $2 \times 2$  stride. The first parallel branch consists of two convolutional layers with batch normalization and ReLU, using a  $3 \times 3$  kernel, 16 depth, and  $1 \times 1$  stride. The next inverted residual segment employs two convolution layers, batch normalization with a depth of 32, a  $3 \times 3$  kernel, and a  $1 \times 1$  stride, activated by ReLU.

The third branch begins with ReLU and includes two convolution layers, two ReLU activations, and a batch normalization layer. These layers use the same padding,  $3 \times 3$  kernels, a  $1 \times 1$  stride, and 64 channels. The complete inverted residual-based architecture appears in **Figure 4**.

### Serial-based feature fusion

Serial feature fusion is a strategy that progressively merges feature maps from multiple layers or model components, enabling the network to capture richer patterns and interdependencies. By aligning features sequentially, the approach enhances representational power—an advantage for tasks such as object detection, segmentation, and video understanding, where diverse and complementary information improves prediction accuracy.

Mathematically, assume two feature matrices  $a$  and  $b$ , each sized  $k \times N$ , where  $k$  denotes the number of features and  $N$  the number of samples.

$$S_{(v)}^{\text{fuse}} = \begin{bmatrix} k \\ N \end{bmatrix} N \times k1 + N \times k2 \quad (1)$$

The most informative DA features are chosen during the fusion stage using an entropy-based selection rule. After this operation, the resulting feature matrices have dimensions of  $N \times 1024$  and  $N \times 1024$ . These fused representations are then passed to the classification module, where neural network-based classifiers determine how many instances fall into each predefined class.

### Feature optimization (BCO)

Khishe and Mosavi (2020) proposed a swarm-based metaheuristic known as the Chimp Optimization Algorithm (ChOA). This method is inspired by the cognitive behaviors and mating-driven strategies of chimpanzees, whose cooperative hunting patterns differ considerably from those of other predatory species. ChOA has been applied in numerous optimization domains because it is straightforward to implement, converges rapidly, avoids premature stagnation, and requires modest computational overhead.

Chimpanzee hunting can be separated into two operational phases: exploration and exploitation. During exploitation, the chimps interact with the prey directly, refining local search in promising regions identified earlier. Exploration, on the other hand, involves scanning the wider environment—chasing, circling, and creating obstacles—to broaden the global search area.

The algorithm models four functional chimp groups: attacker, barrier, chaser, and driver. In the optimization process, each chimp represents a potential solution within the search domain. The attacker corresponds to the best solution found so far, followed by the barrier (second best), the chaser (third), and the driver (fourth). These four elite chimps—denoted as *aattacker*, *abarrier*, *achaser*, and *adriver*—direct how the remaining chimp population *achimp* updates its position at the beginning and end of every iteration. Their influence is computed using the following mathematical expressions.

$$x1^{(t+1)} = a_{\text{attacker}}(t) - A1. (D_{\text{attacker}}), D_{\text{attacker}} = C1. x_{\text{attacker}} - m. x_{\text{chimp}}(t) \quad (2)$$

$$x2^{(t+1)} = a_{\text{barrier}}(t) - A2. (D_{\text{barrier}}), D_{\text{barrier}} = C2. x_{\text{barrier}} - m. x_{\text{chimp}}(t) \quad (3)$$

$$x3^{(t+1)} = a_{\text{chaser}}(t) - A3. (D_{\text{chaser}}), D_{\text{chaser}} = C3. x_{\text{chaser}} - m. x_{\text{chimp}}(t) \quad (4)$$

$$x4^{(t+1)} = a_{\text{driver}}(t) - A4. (D_{\text{driver}}), D_{\text{driver}} = C4. x_{\text{driver}} - m. x_{\text{chimp}}(t) \quad (5)$$

$$x_{\text{chimp}}(t+1) = \frac{a1 + a2 + a3 + a4}{4} \quad (6)$$

Here, *xchimp* represents the position of each candidate solution at iteration  $t$ , where  $t$  denotes the current iteration number.

---

```

Input: The population size  $N$  and total number of iterations  $t$ 
Initialize the population  $X_i (i = 1, 2, \dots, N)$ 
1: while  $t < t_{max-iter}$  do
2:   for each member do
3:     Define the crowd
4:     By using its group strategy to update
5:   end for
6:   for each member do
7:     if  $x < 1$  then
8:       Update the position of current member.
9:     else
10:      if  $w > 1$  then
11:        Select a random number
12:      end if
13:    end if
14:    Update the position of current member.
15:  end for
16:   $X \approx$  Attacker, Barrier, Driver and Chaser
17:   $t + 1$ 
18: end while
19: Return  $X_{attacker}$ 

```

---

**Algorithm 1.** Pseudo-code of the ChOA algorithm.

## Results and Discussion

This section presents a comprehensive discussion of the experimental findings from the proposed framework. Experiments were carried out using medicinal plant image datasets. Each dataset was split evenly, with 50% of images allocated for training and 50% for testing the proposed model. All experiments employed 10-fold cross-validation to balance computational cost and variance, ensuring reliable performance estimation. The feature set used had dimensions of  $\times 1024$ ; the choice of  $k=10$  provided optimal performance, as lower values were insufficient. Each experimental run involved ten iterations of k-fold cross-validation. The models were trained using the following parameters: optimizer SGDM, mini-batch size 16, learning rate 0.0001, and 10 epochs. Performance metrics evaluated included computation time, F1-score, precision, recall, accuracy, error rate, and false-negative rate. All tests were executed on an MSI Leopard motherboard with an Intel Core i7 CPU, 16 GB RAM, 512 GB SSD + 1 TB HDD, and an NVIDIA RTX 4 GB GPU.

### *Results for proposed residual block architecture*

This section presents results obtained from the medicinal plant dataset using the residual block-based CNN architecture. The Residual Block CNN results are summarized in **Table 1**. Among the classifiers, the WNN classifier achieved the highest performance with 99.7% accuracy. Precision, recall, and F1-score were 99.6%, 99.6%, and 99.6%, respectively, with a computational time of 669.05 s. The NNN classifier reached 85.8% accuracy, with a precision and F1-score of 85.7% and 85.8%, respectively. Computational times for classifiers were 543.94 s, 637.68 s, 583.3 s, and 596.99 s. The confusion matrix for the WNN classifier is depicted in **Figure 5**.

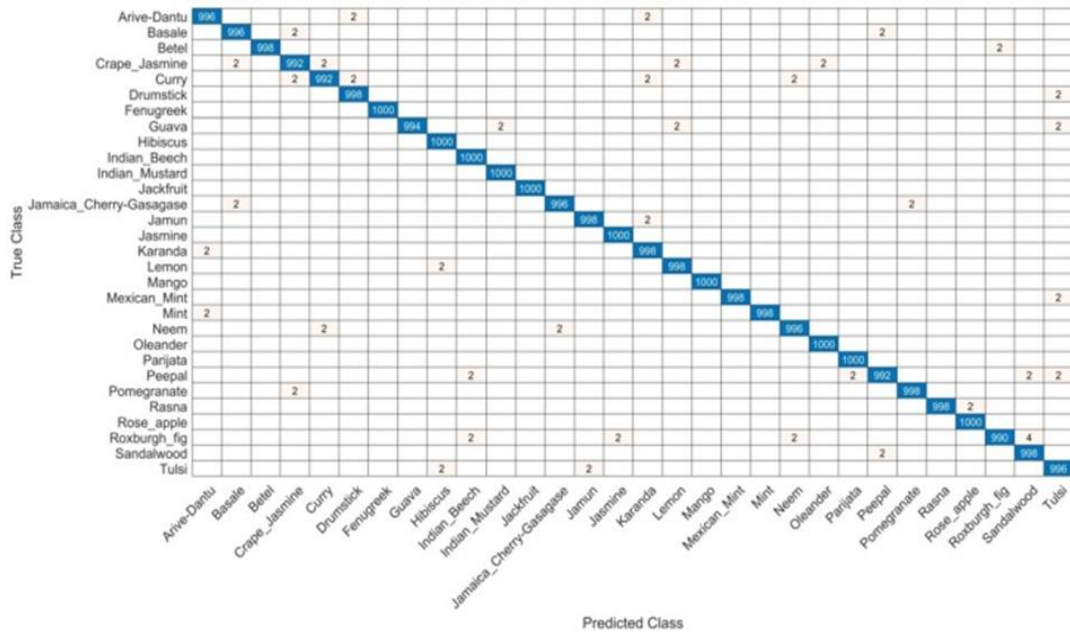


Figure 5. Confusion matrix of WNN classifier for residual block architecture.

Table 1. Results for proposed residual block CNN.

Classifier	Accuracy	Recall	Precision	F1-Score	Computation Time (s)
NNN	85.7	85.8	85.7	85.8	543.94(s)
MNN	98.2	98.1	98.2	98.2	637.68(s)
<b>WNN</b>	<b>99.6</b>	<b>99.6</b>	<b>99.6</b>	<b>99.7</b>	<b>669.05(s)</b>
BNN	84.2	84.1	84.1	84.4	583.3(s)
TNN	82.3	82.4	82.3	82.4	596.99(s)

Results for proposed inverted residual block architecture

This section shows findings from the medicinal plant dataset using the inverted residual block CNN architecture. Results are summarized in Table 2. The WNN classifier again outperformed others, reaching 99.9% accuracy. With a computation time of 343.74 s, accuracy, recall, and F1-score were 99.8%, 99.9%, and 99.8%, respectively. For other classifiers, the NNN achieved 97.6% accuracy, with a precision, recall, and F1-score of 97.5%, 97.6%, and 97.5%. Computational times for classifiers were 597.91 s, 312.98 s, 638.96 s, and 647.99 s. The confusion matrix for WNN is shown in Figure 6.

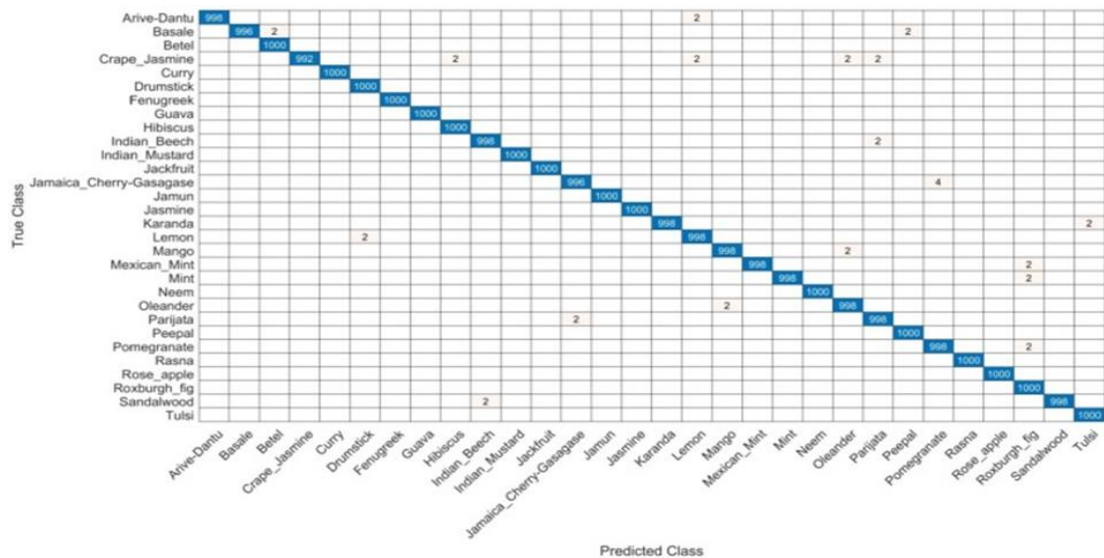


Figure 6. Confusion matrix of WNN classifier for inverted residual block architecture.

**Table 2.** Results for the proposed inverted residual block CNN.

NNN	<b>97.5</b>	<b>97.6</b>	<b>97.5</b>	<b>97.6</b>	<b>597.91(s)</b>
MNN	99.7	99.8	99.7	99.8	312.98(s)
<b>WNN</b>	<b>99.8</b>	<b>99.9</b>	<b>99.8</b>	<b>99.9</b>	<b>343.74(s)</b>
BNN	96.4	96.5	96.5	96.9	638.96(s)
TNN	95.2	95.1	95.1	95.3	647.99(s)

*Serial-based feature fusion results*

Results for serial-based feature fusion are presented in this section. The fused features are derived from the proposed method, combining multiple feature streams. **Table 3** summarizes the performance. The WNN classifier achieved 99.6% accuracy, with a recall and F1-score of 99.5% and 99.6%, respectively, at a computation time of 1586.5 s. Other classifiers recorded accuracies as follows: NNN 85.3%, MNN 98.1%, BNN 84.7%, and TNN 81.2%. Computational times for these classifiers were 1328.2 s, 1534.4 s, 1233 s, and 1274.7 s. **Figure 7** displays the WNN confusion matrix.

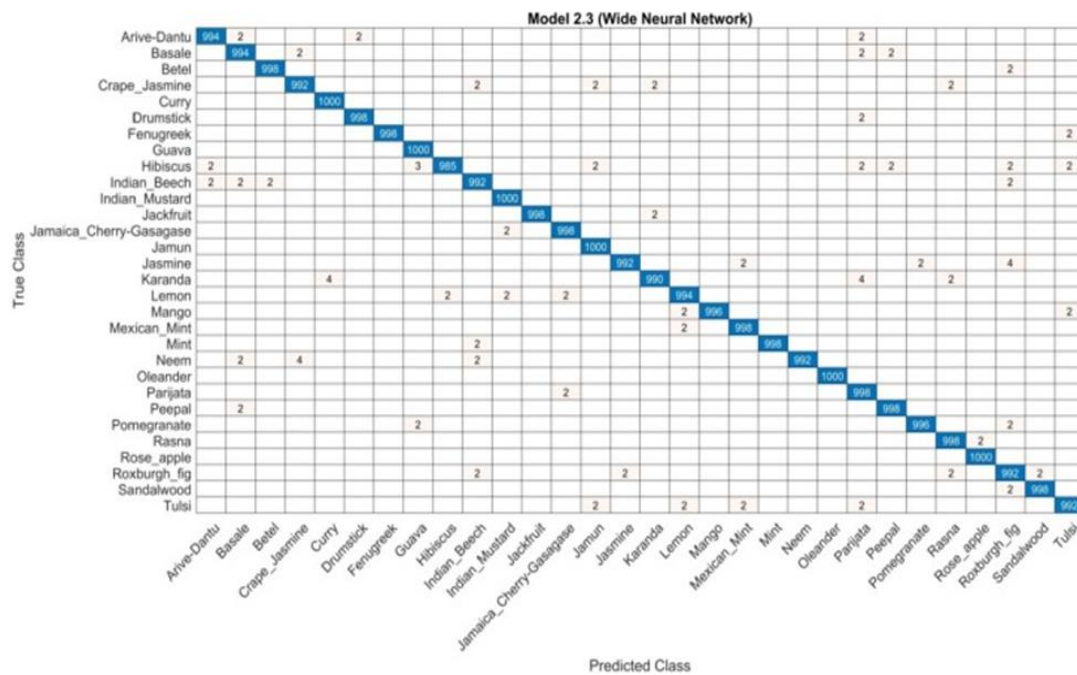


**Figure 7.** Confusion matrix for serial-based feature fusion with WNN classifier.

**Table 3.** Serial-based feature fusion results.

NNN	<b>85.3</b>	<b>85.2</b>	<b>85.3</b>	<b>85.3</b>	<b>1328.2(s)</b>
MNN	97.9	98.0	98.1	98.1	1534.4(s)
<b>WNN</b>	<b>99.5</b>	<b>99.4</b>	<b>99.6</b>	<b>99.6</b>	<b>1586.5(s)</b>
BNN	84.5	84.6	84.7	84.7	1233(s)
TNN	81.1	81.0	81.2	81.2	1274.7(s)

*Feature optimization results*

Finally, the outcomes of feature optimization on the medicinal plant dataset are reported. **Table 4** presents the results of BCO-based feature selection. The WNN classifier remained optimal with 99.6% accuracy, a recall of 99.5%, and an F1-score of 99.6%, with a computation time of 1397.2 s. For other classifiers, precision values were 80.0% for NNN, 93.1% for MNN, 79.6% for BNN, and 77.0% for TNN. Corresponding computational times were 1048.7 s, 1190.5 s, 996.73 s, and 1020.6 s. The WNN classifier confusion matrix is illustrated in **Figure 8**.

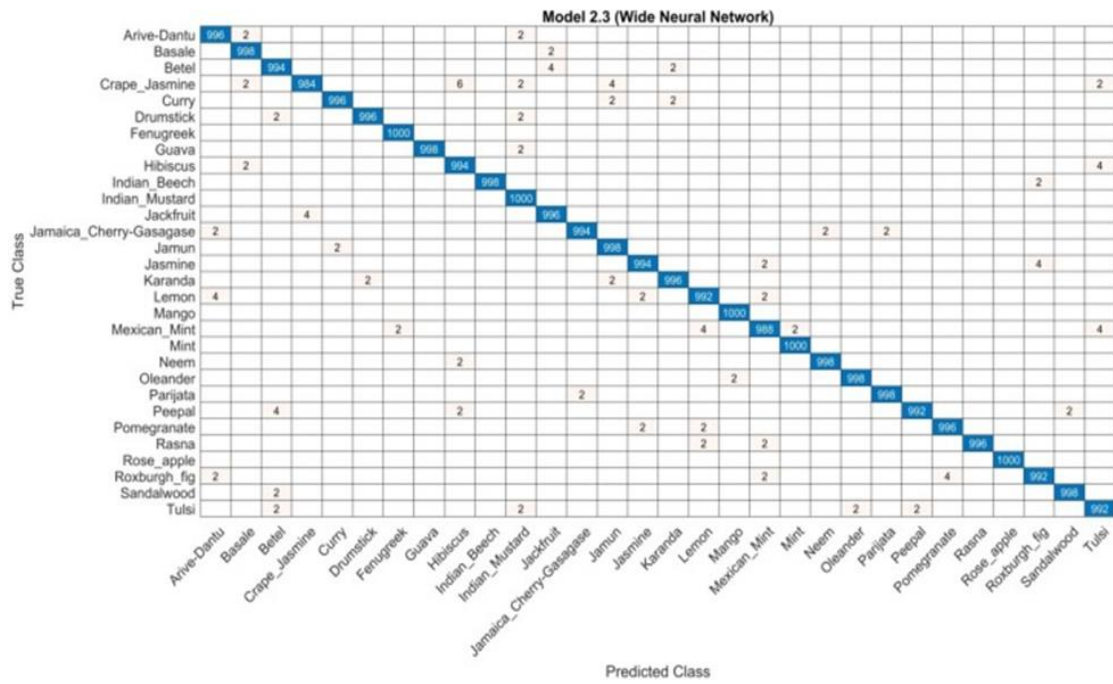


**Figure 8.** Confusion matrix of WNN classifier after feature optimization.

**Table 4.** Feature optimization results.

NNN	79.9	79.8	79.8	80.0	1048.7(s)
MNN	93.0	93.1	93.1	93.1	1190.5(s)
<b>WNN</b>	<b>99.5</b>	<b>99.4</b>	<b>99.6</b>	<b>99.6</b>	<b>1397.2(s)</b>
BNN	79.5	79.6	79.6	79.6	996.73(s)
TNN	77.0	77.0	77.0	77.0	1020.6(s)

#### Grad-CAM visualization

The final step involves visualizing the behavior of the proposed deep learning framework using Grad-CAM. The gradient-based class activation mapping, presented in **Figure 9**, highlights important regions in the input images that contribute most to the model's predictions. The heatmap overlays emphasize these critical areas, with the color brown indicating regions most influential in determining the correct class. This visualization confirms that the proposed model accurately identifies the correct categories.

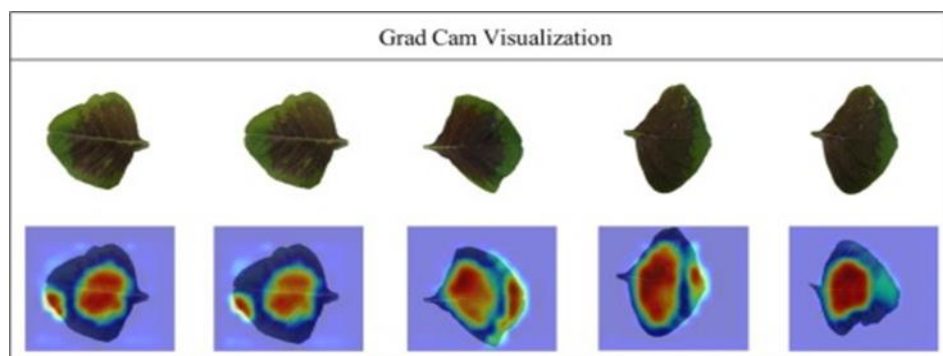


**Figure 9.** Grad-CAM visualization of the proposed deep learning model.

#### Conclusion

This study underscores the vital importance of medicinal plants in healthcare and emphasizes the need for precise classification techniques to ensure their preservation and effective utilization. The use of deep learning, particularly transfer learning methods, demonstrated substantial improvements in classification accuracy and

reliability. Employing advanced CNN architectures, including residual and inverted residual blocks, further enhanced the performance of the classification system. These results highlight the potential of integrating machine learning with botanical research to support biodiversity conservation and optimize the application of medicinal flora in health management.

Future directions include incorporating multimodal data, such as combining leaf images with chemical composition and genetic information, to enhance classification precision and enable differentiation between closely related species. Efforts will also focus on developing models robust to varying environmental conditions, including changes in illumination, backgrounds, and plant maturity, to improve generalization. Expanding the dataset to cover less-represented species and conducting cross-regional studies will provide a more comprehensive classification framework. Finally, these sophisticated classification methods can be deployed in mobile apps or real-time field devices, creating practical tools for researchers, practitioners, and conservationists to identify and preserve medicinal plants in their natural habitats.

**Acknowledgments:** None

**Conflict of Interest:** None

**Financial Support:** None

**Ethics Statement:** None

## References

1. Dileep M, Pournami P, Nair S, Menon A, Jose R, Varghese T. Ayurleaf: a deep learning approach for classification of medicinal plants. In: TENCON 2019 - 2019 IEEE Region 10 Conference (TENCON). IEEE; 2019:321-5
2. Das S, Sardar TH, Sahana D, Mukherjee P, Roy S, Banerjee A. An ensemble technique using genetic algorithm and deep learning for the prediction of rice diseases. In: Machine Learning Hybridization and Optimization for Intelligent Applications. CRC Press; 2025:289-303
3. Duong-Trung N, Quach LD, Nguyen MH, Nguyen CN, Tran QH, Le DT. A combination of transfer learning and deep learning for medicinal plant classification. In: Proc 2019 4th Int Conf Intell Inf Technol. 2019:83-90
4. Amuthalingeswaran C, Sivakumar M, Renuga P, Alexpandi S, Elamathi J, Hari SS. Identification of medicinal plants and their usage by using deep learning. In: 2019 3rd Int Conf Trends Electron Inform (ICOEI). IEEE; 2019:886-90
5. Hicham B, Neşet N, Khedidja B, Leila BS, Talia S, Abderahmane M. The evaluation of *Hertia cheirifolia* L. extract by GC-MS coupled with in silico study as potent inhibitors of human pancreatic lipase. *J Biomol Struct Dyn*. 2024;1-12
6. Rao RU, Lahari MS, Sri KP, Srujana KY, Yaswanth D, Reddy P. Identification of medicinal plants using deep learning. *Int J Res Appl Sci Eng Technol*. 2022;10:306-22
7. Abdollahi J, Ahmadi S, Karimi R, Mohammadi A, Farhadi M, Rezaei H. Identification of medicinal plants in Ardabil using deep learning. In: 2022 27th Int Comput Conf Comput Soc Iran (CSICC). IEEE; 2022:1-6
8. Hicham B, Djeridane A, Mahfoudi R, Benali K, Ouzidane F, Bouziane M. Xanthine oxidase inhibitory activity and uric acid dissolution power of some plant extracts: in vitro therapeutical approach for gout treatment. *Rev Bras Farmacogn*. 2024;34:1340-52
9. Aissa NEHSB, Korichi A, Lakas A, Kerrache CA, Calafate CT, Boukhalfa K. Assessing robustness to adversarial attacks in attention-based networks: case of EEG-based motor imagery classification. *SLAS Technol*. 2024;100142
10. Mulugeta AK, Sharma DP, Mesfin AH, Patel S, Kumar R, Singh V. Deep learning for medicinal plant species classification and recognition: a systematic review. *Front Plant Sci*. 2024;14:1286088
11. Deshmukh M, Patil S, Kulkarni R, Joshi A, Naik P, Shah D. Deep learning for the classification and recognition of medicinal plant species. *Indian J Inf Sci Technol*. 2024;17(11):1070-7

12. Aissa NEHSB, Lakas A, Korichi A, Kerrache CA, Belkacem AN, Bouzid M. Robust detection of adversarial attacks for EEG-based motor imagery classification using hierarchical deep learning. In: 15th Int Conf Innov Inf Technol (IIT). IEEE; 2023:156-61
13. Ghosh S, Singh A, Kumar S, Chatterjee P, Das R, Sen A. PB3C-CNN: an integrated PB3C and CNN based approach for plant leaf classification. *Intell Artif.* 2023;26(72):15-29
14. Wu SG, Bao FS, Xu EY, Wang YX, Chang YF, Zhang QL. A leaf recognition algorithm for plant classification using probabilistic neural network. In: 2007 IEEE Int Symp Signal Process Inf Technol. IEEE; 2007:11-6
15. Herdiyeni Y, Wahyuni NKS, Pratama R, Sari D, Wibowo A, Lestari N. Mobile application for Indonesian medicinal plants identification using fuzzy local binary pattern and fuzzy color histogram. In: Int Conf Adv Comput Sci Inf Syst (ICACSIS). IEEE; 2012:301-6
16. Ma LH, Zhao ZQ, Wang J, Liu Y, Chen X, Zhang H. Apleafis: an Android-based plant leaf identification system. In: Int Conf Intell Comput. Springer; 2013:106-11
17. Grinblat GL, Uzal LC, Larese MG, Granitto PM, Fernández R, Pizarro R. Deep learning for plant identification using vein morphological patterns. *Comput Electron Agric.* 2016;127:418-24
18. Paulson A, Ravishankar S, Menon D, Kumar P, Nair V, Suresh R. AI based indigenous medicinal plant identification. In: 2020 Adv Comput Commun Technol High Perform Appl (ACCTHPA). IEEE; 2020:57-63
19. Nasiri A, Taheri-Garavand A, Fanourakis D, Zhang YD, Nikoloudakis N, Papadopoulos S. Automated grapevine cultivar identification via leaf imaging and deep convolutional neural networks: a proof-of-concept study employing primary Iranian varieties. *Plants.* 2021;10(8):1628
20. Hu J, Chen Z, Yang M, Zhang R, Cui Y, Li X. A multiscale fusion convolutional neural network for plant leaf recognition. *IEEE Signal Process Lett.* 2018;25(6):853-7